Poster Contributions

https://doi.org/10.1017/S1743921318006919 Published online by Cambridge University Press

Dwarf Galaxies: From the Deep Universe to the Present
Proceedings IAU Symposium No. 344, 2019
K. B. W. McQuinn & S. Stierwalt, eds.

doi:10.1017/S1743921318006919

Census of Lyα, [OIII]5007, Hα, and [CII]158μm Line Emission with $\sim$1000 Low-mass Lyman Alpha Emitters at $z = 4.9 - 7.0$ Revealed with Subaru/Hyper-Suprime Cam Survey

Yuichi Harikane[1,2]

[1]Institute for Cosmic Ray Research, The University of Tokyo, 5-1-5 Kashiwanoha, Kashiwa, Chiba 277-8582, Japan

[2]Department of Physics, Graduate School of Science, The University of Tokyo, 7-3-1 Hongo, Bunkyo, Tokyo, 113-0033, Japan
email: hari@icrr.u-tokyo.ac.jp

Abstract. We investigate Lyα, [OIII]λ5007, Hα, and [CII]158μm emission from 1,124 low-mass galaxies (typically $M_* \sim 10^8$ M$_\odot$) at $z = 4.9 - 7.0$, composed of 1,092 Lyα emitters (LAEs) at $z = 4.9 - 7.0$ identified by Subaru/Hyper Suprime-Cam (HSC) narrowband surveys and 34 galaxies at $z = 5.148 - 7.508$ with deep ALMA [CII]158μm data in the literature. At $z = 4.9$, we find that the rest-frame Hα equivalent width positively correlates with the rest-frame Lyα equivalent width $EW^0_{\rm Ly\alpha}$. At $z = 5.7 - 7.0$, there exists an interesting turn-over trend that the [OIII]/Hα flux ratio increases in $EW^0_{\rm Ly\alpha} \simeq 0 - 30$ Å, and then decreases out to $EW^0_{\rm Ly\alpha} \simeq 130$ Å. We also identify an anti-correlation between a [CII] luminosity to star-formation rate ratio ($L_{\rm [CII]}/SFR$) and $EW^0_{\rm Ly\alpha}$ at the > 99% confidence level. We carefully investigate physical origins of the correlations, and find that a simple anti-correlation between $EW^0_{\rm Ly\alpha}$ and metallicity explains self-consistently all of the relations identified in our study.

1. Introduction

Probing physical conditions of the inter-stellar medium (ISM) is fundamental in understanding star formation and gas reprocessing in galaxies across cosmic time. Early ALMA observations found surprisingly weak [CII]158μm emission in Lyα emitters (LAEs) at $z \sim 6 - 7$ ([CII] deficit; e.g., Ouchi *et al.* (2013); Ota *et al.* (2014); Schaerer *et al.* (2015); Maiolino *et al.* (2015)). A theoretical study discusses that the [CII] deficit can be explained by very low metallicity (0.05 $Z_\odot$) in the ISM (Vallini *et al.* (2015); Olsen *et al.* (2017)). Thus estimating metallicities of the high-redshift galaxies is crucial to our understanding of the origin of the [CII] deficit.

The ISM property is also important for cosmic reionization. Observations by the Planck satellite and high redshift UV luminosity functions (LFs) suggest that faint and abundant star-forming galaxies dominate the reionization process (e.g., Robertson *et al.* (2015)), and understanding ionizing properties of such star forming galaxies is important. Various studies constrain ionizing photon production efficiencies of star forming galaxies to be $\log\xi_{\rm ion}/[{\rm Hz\ erg^{-1}}] = 24.8 - 25.3$ at $z \sim 0 - 2$ (e.g., Matthee *et al.* (2017); Izotov *et al.* (2017); Shivaei *et al.* (2017); see also Sobral *et al.* (2018)). Since the faint star-forming galaxies are expected to be strong line emitters, it is important to estimate $\xi_{\rm ion}$ of LAEs at higher redshift, as their ISM properties are likely more similar to the ionizing sources.

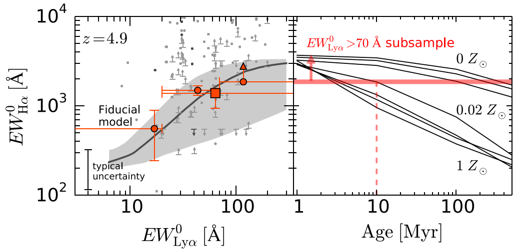

Figure 1. Left panel: Hα EWs as a function of Lyα EWs at $z=4.9$. The red square and circles are the results from the stacked images of the subsamples, and the gray dots show the EWs of the individual objects detected in the [3.6] and/or [4.5] bands. The dark and light gray dots are objects spectroscopically confirmed and not, respectively. The upward and downward arrows represent the 2σ lower and upper limits, respectively. The dark gray curve and the shaded region show the prediction from the fiducial model. **Right panel:** Inferred stellar age and metallicity from the constrained $EW^0_{\mathrm{H}\alpha}$. The red solid line shows the lower limit of $EW^0_{\mathrm{H}\alpha} \gtrsim 2000$ Å in the 70 Å $< EW_{\mathrm{Ly}\alpha} <$ 1000 Å subsample at $z=4.9$. The black curves represent $EW^0_{\mathrm{H}\alpha}$ calculated in Inoue (2011) with metallicities of $Z=0$, 5×10^{-6}, 5×10^{-4}, 0.02, 0.2, 0.4, and 1 $Z_\odot$.

2. Data & Analysis

We use LAE samples at $z=4.9$, 5.7, 6.6, and 7.0 selected with the NB filters of $NB718$, $NB816$, $NB921$, and $NB973$, respectively (Shibuya *et al.* (2018); Itoh *et al.* (2018) Zhang et al. in prep.), obtained in our Subaru/Hyper Suprime-Cam (HSC) survey (Aihara *et al.* (2018a) Aihara *et al.* (2018b)). We divide our LAE samples into subsamples by the Lyα equivalent width (EW) bins. We cut out 12" × 12" images of the LAEs in HSC $grizyNB718NB816NB921NB973$ ($grizyNB816NB921$), VIRCAM JHK_s (WFCAM JHK), and IRAC [3.6][4.5] bands in the UD-COSMOS (UD-SXDS) field. Then we generate median-stacked images of the subsamples in each band.

We generate the model SEDs at $z=4.9$, 5.7, 6.6, and 7.0 using BEAGLE (Chevallard & Charlot (2016)). We estimate rest-frame optical emission line fluxes by comparing the stacked SEDs with the model SEDs. We calculate the flux differences between the stacked SEDs and the model SEDs in the [3.6] band at $z=4.9$, and [3.6] and [4.5] bands at $z=5.7$, 6.6, and 7.0. The flux differences are corrected for dust extinction with the τ_{V} values in the models, assuming the Calzetti *et al.* (2000) extinction curve. We estimate the Hα, Hβ, and [OIII]λ5007 line fluxes from these flux differences.

In addition to our HSC LAE samples, we compile previous ALMA and PdBI observations targeting [CII]158μm in galaxies at $z>5$. We use results of 34 galaxies from the literature (see Table 3 in Harikane *et al.* (2018)).

3. Results

The left panel in Figure 1 shows rest-frame Hα EWs ($EW^0_{\mathrm{H}\alpha}$) as a function of Lyα EWs at $z=4.9$. The Hα EW increases from ~ 600 Å to >1900 Å with increasing Lyα EW. This high $EW^0_{\mathrm{H}\alpha}$ value indicates very young stellar age of <10 Myr or very low metallicity of $<0.02\ Z_\odot$ (the right panel in Figure 1).

We estimate the ionizing photon production efficiencies of the $z=4.9$ LAEs from their Hα fluxes and UV luminosities. The left panel in Figure 2 shows estimated ξ_{ion} values as a function of UV magnitude. We calculate the values of the ξ_{ion} in two cases; $f^{\mathrm{ion}}_{\mathrm{esc}}=0$ and $f^{\mathrm{ion}}_{\mathrm{esc}}=0.1$. The ionizing photon production efficiency is estimated to be $\log\xi_{\mathrm{ion}}/[\mathrm{Hz\ erg^{-1}}]=25.48^{+0.06}_{-0.06}$ for the $EW^0_{\mathrm{Ly}\alpha}>20$ Å subsample with $f^{\mathrm{ion}}_{\mathrm{esc}}=0$. This value is systematically higher than those of LBGs at the similar redshift and UV magnitude ($\log\xi_{\mathrm{ion}}/[\mathrm{Hz\ erg^{-1}}]\simeq 25.3$; Bouwens *et al.* (2016)) by $60-100\%$.

https://doi.org/10.1017/S1743921318006919 Published online by Cambridge University Press

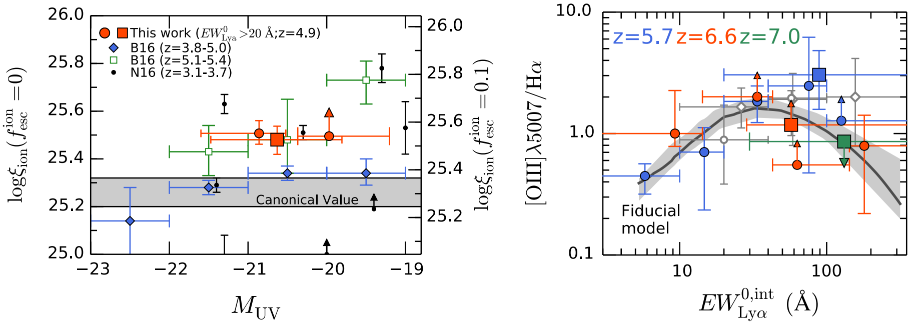

Figure 2. Left panel: Inferred ionizing photon production efficiencies of the LAEs at $z = 4.9$ as a function of UV magnitude. The left and right axes represent the efficiencies with the ionizing photon escape fractions of 0 and 10%, respectively. The red circles and square show the results of the subsamples divided by $EW^0_{Ly\alpha}$, and the upward arrow represents the 2σ lower limit. The ξ_{ion} values of LBGs at $z = 3.8 - 5.0$ in Bouwens *et al.* (2016) are represented as the blue diamonds. We plot the ξ_{ion} values of LBGs at $z = 5.1 - 5.4$ (Bouwens *et al.* (2016)) and LAEs at $z = 3.1 - 3.7$ (Nakajima *et al.* (2016)) with the green open squares and black circles, respectively. The gray shaded region indicates typically assumed ξ_{ion} (see Table 2 Bouwens *et al.* (2016)). **Right panel:** [OIII]/Hα ratio as a function of the Lyα EW. The blue, red, and green circles and squares are the [OIII]λ5007/Hα flux ratios at $z = 5.7$, 6.6, and 7.0, respectively. The open gray diamonds and circles are the ratios of $z = 2.5$ and 0.3 galaxies (Trainor *et al.* (2016); Cowie *et al.* (2011)), respectively. We also plot the fitting result of the $(Z, \log U, \mathrm{Age}) - EW^0_{Ly\alpha}$ relations with the dark gray curve with the shaded region representing the 1σ uncertainty.

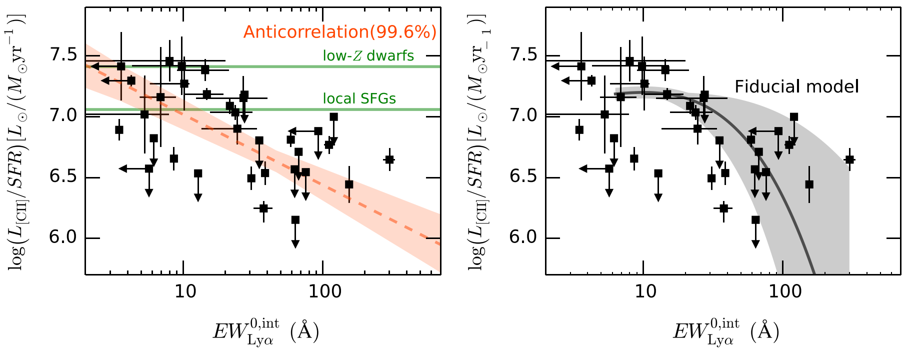

Figure 3. Left panel: Ratio of the [CII] luminosity to the SFR as a function of rest-frame Lyα EW. We plot the results of the previous ALMA and PdBI observations of $z > 5$ galaxies. We find the anti-correlation in the $L_{[CII]}/SFR - EW^{0,int}_{Ly\alpha}$ plane at the 99.6% confidence level. The green horizontal lines show the $L_{[CII]}/SFR$ ratios for low-metallicity dwarf galaxies and local star-forming galaxies in De Looze *et al.* (2014) for $SFR = 10$ $M_\odot yr^{-1}$. The red-dashed line and the shaded region denote the best-fit $L_{[CII]}/SFR - EW^{0,int}_{Ly\alpha}$ relation. **Right panel:** Same as the left panel but with the prediction from the fiducial model. The dark gray curve and the shaded region represent the prediction from the fiducial model and its 1σ uncertainty, respectively.

The [OIII]/Hα ratios of the $z = 5.7$, 6.6, and 7.0 LAEs are presented in the right panel in Figure 2. We find that the ratio increases with increasing $EW^0_{Ly\alpha}$ from 7 Å to 20 Å, then decreases to ~ 130 Å, showing the turn-over trend at the 2.3σ confidence level.

In the left panel in Figure 3, we plot the ratios of the [CII] luminosity to SFR, $L_{[CII]}/SFR$ as a function of Lyα EW corrected for the IGM absorption, $EW^{0,int}_{Ly\alpha}$. We find an anti-correlation in the $L_{[CII]}/SFR - EW^{0,int}_{Ly\alpha}$ plane at the 99.6% confidence level.

https://doi.org/10.1017/S1743921318006919 Published online by Cambridge University Press

4. Discussion

We investigate physical quantities explaining our observed [OIII]/Hα ratios as a function of Lyα EW. We simply parameterize the metallicity, $Z_{\rm neb}$, the ionization parameter, $U_{\rm ion}$, and the stellar age with the Lyα EW in units of Å. We fit our observational results of the [OIII]/Hα ratios with this model, and the best-fit relations with 1σ errors are

$$\log Z_{\rm neb} = -0.33^{+0.16}_{-0.11}(\log EW^{0,\rm int}_{\rm Ly\alpha})^2 + 0.35^{+0.10}_{-0.18}, \tag{4.1}$$

$$\log U_{\rm ion} = -0.09^{+0.66}_{-0.22}\log EW^{0,\rm int}_{\rm Ly\alpha} - 2.58^{+0.33}_{-0.81}, \tag{4.2}$$

$$\log{\rm Age} = -0.29^{+1.66}_{-0.77}\log EW^{0,\rm int}_{\rm Ly\alpha} + 8.90^{+0.47}_{-3.21}. \tag{4.3}$$

The result suggests an anti-correlation between the metallicity and the Lyα EW, implying the very metal-poor ISM ($\sim 0.03\ Z_\odot$) in the galaxies with $EW^{0,\rm int}_{\rm Ly\alpha} \sim 200$ Å (see also; Nagao *et al.* (2007); Hashimoto *et al.* (2017)). Hereafter, we call this model "the fiducial model". We find that this fiducial model agrees well with the observed $EW^0_{\rm H\alpha} - EW^0_{\rm Ly\alpha}$ relation (the left panel in Figure 1). The fiducial model can also nicely explains the $L_{\rm [CII]}/SFR - EW^{0,\rm int}_{\rm Ly\alpha}$ anti-correlation (the right panel in Figure 3), indicating that the [CII] deficit in high Lyα EW galaxies may be due to the low metallicity.

References

Aihara, H., Armstrong, R., Bickerton, S., *et al.* 2018a, *PASJ*, 70, S8
Aihara, H., Arimoto, N., Armstrong, R., *et al.* 2018b, *PASJ*, 70, S4
Bouwens, R. J., Smit, R., Labbé, I., *et al.* 2016, *ApJ*, 831, 176
Calzetti, D., Armus, L., Bohlin, R. C., *et al.* 2000, *ApJ*, 533, 682
Chevallard, J., & Charlot, S. 2016, *MNRAS*, 462, 1415
Cowie, L. L., Barger, A. J., & Hu, E. M. 2011, *ApJ*, 738, 136
De Looze, I., Cormier, D., Lebouteiller, V., *et al.* 2014, *A&A*, 568, A62
Harikane, Y., Ouchi, M., Shibuya, T., *et al.* 2018, *ApJ*, 859, 84
Hashimoto, T., Ouchi, M., Shimasaku, K., *et al.* 2017, *MNRAS*, 465, 1543
Inoue, A. K. 2011, *MNRAS*, 415, 2920
Itoh, R., Ouchi, M., Zhang, H., *et al.* 2018, ArXiv e-prints, arXiv:1805.05944
Izotov, Y. I., Guseva, N. G., Fricke, K. J., Henkel, C., & Schaerer, D. 2017, *MNRAS*, 467, 4118
Maiolino, R., Carniani, S., Fontana, A., *et al.* 2015, *MNRAS*, 452, 54
Matthee, J., Sobral, D., Best, P., *et al.* 2017, *MNRAS*, 465, 3637
Nagao, T., Murayama, T., Maiolino, R., *et al.* 2007, *A&A*, 468, 877
Nakajima, K., Ellis, R. S., Iwata, I., *et al.* 2016, *ApJ*l, 831, L9
Olsen, K., Greve, T. R., Narayanan, D., *et al.* 2017, *ApJ*, 846, 105
Ota, K., Walter, F., Ohta, K., *et al.* 2014, *ApJ*, 792, 34
Ouchi, M., Ellis, R., Ono, Y., *et al.* 2013, *ApJ*, 778, 102
Robertson, B. E., Ellis, R. S., Furlanetto, S. R., & Dunlop, J. S. 2015, *ApJ*l, 802, L19
Schaerer, D., Boone, F., Zamojski, M., *et al.* 2015, *A&A*, 574, A19
Shibuya, T., Ouchi, M., Konno, A., *et al.* 2018, *PASJ*, 70, S14
Shivaei, I., Reddy, N. A., Siana, B., *et al.* 2017, ArXiv e-prints, arXiv:1711.00013
Sobral, D., Santos, S., Matthee, J., *et al.* 2018, *MNRAS*, arXiv:1712.04451
Trainor, R. F., Strom, A. L., Steidel, C. C., & Rudie, G. C. 2016, *ApJ*, 832, 171
Vallini, L., Gallerani, S., Ferrara, A., Pallottini, A., & Yue, B. 2015, *ApJ*, 813, 36

https://doi.org/10.1017/S1743921318006919 Published online by Cambridge University Press